Numerical Simulations of Stiffened Multi-arch Double-layered Panels Subjected to Blast Loading

Wensu Chen* **and Hong Hao**
Tianjin University and the University of Western Australia Joint Research Center of Protective Structures;
School of Civil and Resource Engineering
The University of Western Australia,
35 Stirling Highway, Crawley, WA 6009, Australia

Received on 26 feb 2013, Accepted on 13 April 2013

ABSTRACT
Blast-resistant structures are traditionally designed and fabricated with solid materials of heavy weight to resist blast loadings. This not only increases the material and construction costs, but also undermines the operational performance of protective structures. To overcome these problems, new designs with either new structural forms or new materials are demanded against blast loads. A multi-arch double-layered panel has been proposed as a new structural form in a previous study (1). Its performance has been numerically demonstrated better than other forms of double-layered panels in resisting blast loads. In this study, to further improve the effectiveness of the multi-arch double-layered panel in resisting blast loads, responses of a five-arch double-layered panel with rectangular stiffeners to detonations are investigated by using finite element code Ls-Dyna. The numerical results show that the stiffened panel outperforms the unstiffened panel of the same weight in terms of the blast-resistant capacity and energy absorption capacity. Parametric studies are conducted to investigate the effects of various stiffener configurations, boundary conditions, stiffener dimension, strain rate sensitivity and blast intensity on the dynamic response to blast loadings. The central point displacements, internal energy absorptions, boundary reaction forces and plastic strains are compared and the optimal configurations of blast-resistant panel are determined. It demonstrates that the strategic arrangement of stiffeners with appropriate boundary conditions can maximize the reduction of dynamic response of the panels to blast loadings. The stiffened multi-arch dotuble-layered panels have great application potentials in the blast-resistant panel design.

Key words: Stiffened panel, Multi-arch double-layered panel, Blast-resistant, Numerical simulation, Ls-Dyna

*Corresponding author. Tel.: +61-8-6488-7420. E-mail address: wensu.chen@uwa.edu.au

1. INTRODUCTION

Protective structures, such as protective panel, are traditionally designed and built in a bulky and solid way, which leads to poor operational performance and high costs [2]. The ideal protective structures should be lightweight while capable of resisting blast loads. A multi-arch unstiffened panel as shown in Figure 1 [1] has been proposed as a new structural form to better resist blast loads. Its performance has been numerically demonstrated better than other forms of double-layered panels in resisting blast loads. This is because the multiple arches cancel out certain blast loads at supports of two adjacent arches and lead to a reduction of the loads transferred to the internal layer and the panel boundary. However, high stress concentrations occur at the springing lines where the front arched layer is connected to the flat internal layer, which has been shown in the experimental and numerical investigations [1]. The elements at these locations are vulnerable and damage at these locations may compromise the overall blast load-carrying capacity of the panel. To mitigate the possible damage due to these stress concentrations, as well as the damage caused by buckling of the front arched layer, stiffeners are considered to be placed at strategic locations to prevent these localized damages and reinforce the panel. These stiffeners are designed to enhance the capacity of the front arch and internal flat layer to prevent bending and buckling failure, thus to improve the overall performance of the multi-arch double-layered panel in resisting blast loads.

Stiffened panels are lightweight and high-strength structural elements, which have been widely used in design and construction of buildings, defence shelters, blast-resistant doors and offshore blast wall panels etc. The behaviors of stiffened panels against blast loadings have been intensively investigated in recent decades. As reported, the stiffened panels have better performance than the unstiffened panels. An optimal layout of stiffeners was determined by comparing three stiffened plates with equivalent unstiffened plate [3]. Possible failure modes were reported by Nurick, et al. [4] after conducting experimental and numerical studies on fully built-in singly stiffened plates under blast loadings. In 2005, the quadrangular plates with five stiffener configurations (e.g. unstiffened, single, double, cross and double cross stiffened) were experimentally and numerically investigated under both uniform and localized blast loadings. Both temperature-dependant material properties and strain rate effect were incorporated in the numerical model. The stiffener configuration was found to have more effect on the response to the localized blast loadings and the

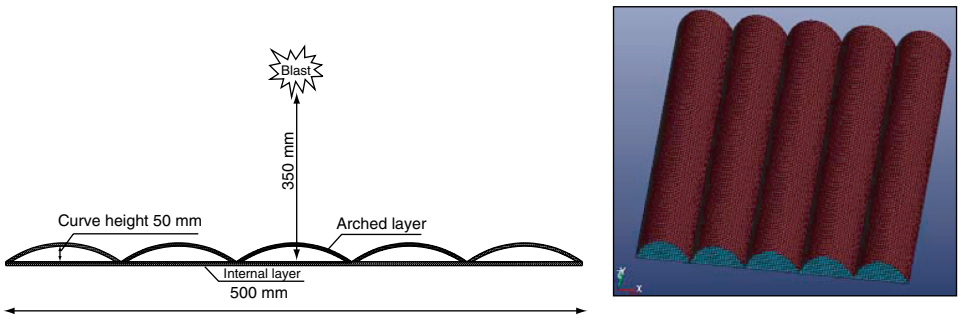

Figure 1. Schematic section diagram and FE model of the unstiffened panel UU

influence of the stiffener size on the performance of stiffened panel was important [5, 6]. Full scale stiffened panels subjected to air-blast explosions have been investigated experimentally and numerically. The numerical results are in good correlation of the experimental results [7]. Numerical study on the clamped, square stiffened plates subjected to blast loading has been presented. The predicted failure modes consider the interaction effects of tensile and bending strain on tearing and shear failure, which has been compared with the experimental data [8]. Goel, et al. [9] conducted numerical investigations to examine the effect of ten stiffener configurations on the dynamic response of rectangular flat plate to blast loadings. It is reported that the stiffener layout and strain rate consideration governed the response of the plates to blast loadings. Hsieh, et al. [10] investigated the blast resistance of a door structure with multiple inter-stiffeners by using finite element analysis and static stiffness experiment. It is shown that the increase of the depth and web thickness of the stiffeners can reduce the deflection of the stiffened door significantly. Pan and Louca [11] carried out experimental and numerical studies on stiffened plates subjected to hydrocarbon explosions. It was reported that the contribution of stiffeners was mainly influenced by the second moment of the cross section. A typical blast wall and a tee-stiffened panel subjected to hydrocarbon explosions were numerically investigated and correlated with the experimental work in [12]. The effects of peak pressure, shape of pressure-time curve and boundary restraints on the response of panel were investigated in the parametric study in [12]. The effects of parameters such as plate slenderness ratio, plate aspect ratio and cross-sectional area ratio on the load carrying capacity and the failure mode of the tee-stiffened panels were also presented in [13].Although many researchers have been studying the stiffened flat panel against blast loads, no investigations into the stiffened multi-arch panels subjected to blast loadings have been reported yet in the literature.

As reviewed above, either experimental tests, or numerical simulations or both are carried out to study the panel responses to blast loads. The experimental testing can demonstrate the overall structural response straightforwardly. However, it has some shortcomings related to the cost, time and safety. Sometimes it is neither feasible nor possible to conduct blasting tests owing to these constraints. Moreover, the reproducibility of blast test results is not always ensured due to the uncertainties involved in blast, and the blast test results often cannot be extrapolated, which greatly limit the applicability of the testing results. On the other hand, reliable numerical simulation overcomes the above shortcomings. It can be used to simulate physical tests and better study the structural dynamic responses. It allows more detailed observations and measurements of structural responses that are often difficult in physical tests, e.g. measurements of the distributions of internal stress and strain of structures are very difficult in experimental tests, but are easily achievable in numerical simulations. However, physical tests cannot be abolished, which are needed to calibrate the numerical model. Only a proven numerical model can be used to simulate physical tests and study the dynamic responses of structures to blast loads.

This study presents numerical simulations to investigate the effect of using rectangular stiffeners in five-arch double-layered panels. Finite element code Ls-Dyna [14] is employed in this study to analyze the blast resistant and energy absorption capacities of the stiffened and unstiffened panels of the same total weight to study the effectiveness of using stiffener in improving the blast load resistance capacities of the double-layered panels. The calibrated numerical model [1] validated by the experimental and numerical data in [15] are used to carry out the simulations in this study. The blast-resistant capacity and energy absorption capacity of the two panel systems are compared. In addition, a series of parametric studies

are carried out to investigate the effects of rectangular stiffener configurations, i.e. stiffener arrangements and stiffener section sizes, boundary conditions and strain rate sensitivity on the structural response of panels to blast loadings. Peak displacement, internal energy absorption, boundary reaction forces and plastic strain are extracted and used as response parameters to compare the effectiveness of various panel configurations on the blast resistance capacities. Based on the numerical simulation results, the optimal configuration of stiffened five-arch double-layered panel is determined. The implementation of this stiffened multi-arch double-layered panel design into civilian protective structures might be considered.

2. PANEL CONFIGURATIONS

Both unstiffened and stiffened panels are made of mild steel with the projected dimensions of 500 mm by 500 mm. The unstiffened panel designated as "UU" ("Unstiffened" on arched layer and "Unstiffened" on flat layer) is a double-layered panel consisting of a flat internal layer and a five-arch layer with the arch surface facing the blast load. The thicknesses of both layers of the unstiffened panel are 2 mm. The arch height is 50 mm. The arched layer is welded to the internal flat layer. To investigate the effect of stiffeners, a panel with rectangular stiffeners placed on arched and flat layers is configured as shown in Figure 2 and designated as "F4". The arched layer of the panel "F4" is arranged with five stiffeners each along the crest of arch surface in Y direction, and three stiffeners at the mid and ends of each arch surface of the arched layer in X direction. The flat layer of "F4" is strengthened with four stiffeners at the springing lines of two arch surfaces in Y direction and two stiffeners along the boundary of the flat layer in X direction. The rectangular stiffeners, 10 mm in width and 5 mm in depth, are placed and welded to the side of layer facing the blast loadings with continous fillet welds. To make the total weight of stiffened panel "F4" approximately the same as the unstiffened panel "UU", the thicknesses of both the front arch and internal flat layers of "F4" are adjusted to 1.39 mm, as indicated in Table 2. The boundary conditions of panels are assumed to be fully fixed around the whole perimeter of the internal flat layer.

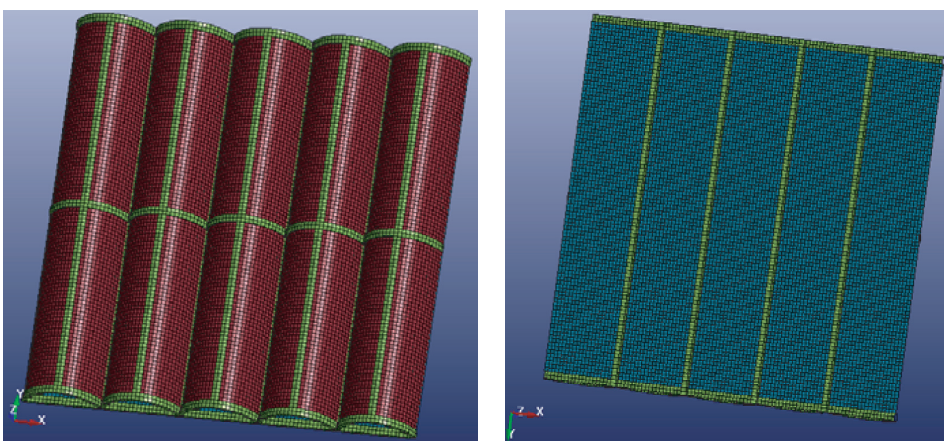

Figure 2. Configuration of the stiffened panel F4 (left: top view; right: bottom view)

3. NUMERICAL SIMULATIONS

The numerical model of steel plate under blast loads is developed in a previous study [1]. The validity of the model is verified by simulating a field blasting test [15]. The same model i.e. material properties, boundary conditions, element sizes and blast loading calculations is used in this study to simulate the responses of stiffened five-arch double-layered panels to blast load. As compared to the calibrated model in [1], the only major difference is the addition of stiffeners. Therefore, the calibrated numerical model is believed reliable to predict the dynamic responses of the stiffened five-arch double-layered panels subjected to blast loads.

3.1. ELEMENT TYPES AND CONNECTIONS

The numerical models are created by using commercial software ANSYS and Ls-Prepost. The Belytschko-Tsay shell element [16] with element size of 5 mm is utilized to model the arched and flat layers of the panels. The fully integrated S/R solid element [16] with element size of 5 mm is used to model the stiffeners. Perfect connections between the front arched and internal flat layers are assumed in the study and modeled as common points. Perfect connections between the stiffeners and the respective layers described above are also assumed and modeled as common points. To prevent the stiffeners penetrating into the arched and flat layers, the keyword *CONTACT AUTOMATIC SINGLE SURFACE is employed with a contact friction value of 0.2.

3.2. MESH CONVERGENCE TEST

The computational accuracy is dependent on the element size. Three element sizes of 2.5 mm, 5 mm and 7.5 mm representing fine, medium and coarse meshes are used for the mesh convergence tests on the panel "F4". Figure 3 shows that the central point displacement time histories of flat layer obtained from the models with different mesh sizes are in close agreement, indicating the chosen mesh sizes lead to similar response of the panel subjected to blast load. Hence, mesh size of 5.0 mm is used in the subsequent calculations.

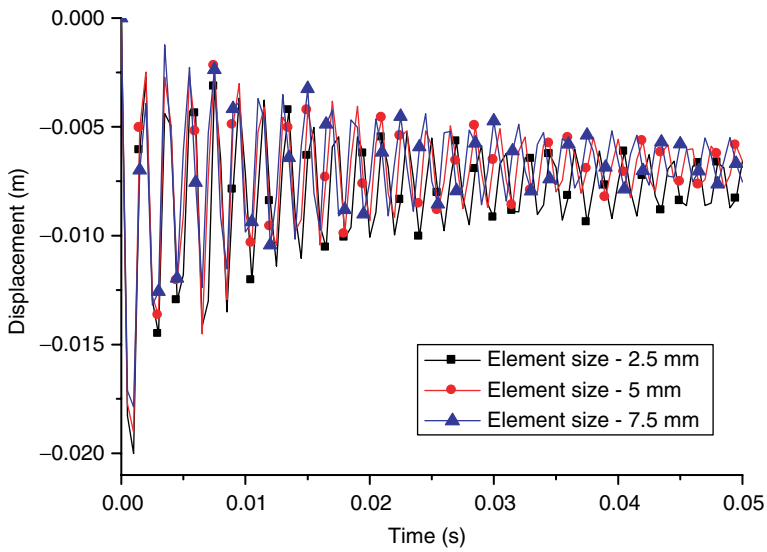

Figure 3. Displacement time histories obtained with different mesh sizes

3.3. MATERIAL MODELS

The elastic-plastic material model *MAT PLASTIC KINEMATIC in Ls-Dyna is adopted to model the steel. It is suitable for modeling the bi-linear elastic-plastic constitutive relation of metals with isotropic kinematic hardening plasticity. The input parameters defined in this material model are based on the quasi-static material testing. The strain rate effect is taken into account by using Cowper-Symonds model available in Ls-Dyna as defined in Eq.(1). It is commonly used to simulate the strain rate effect of structure steels [5, 17]. To demonstrate the strain rate effect, the model without considering strain rate effect is also analyzed in section 4.5.

$$\frac{\sigma_d}{\sigma_s} = 1 + \left(\frac{\dot{\varepsilon}}{C}\right)^{1/p} \tag{1}$$

where σ_d is the dynamic yield stress at plastic strain rate $\dot{\varepsilon}$, σ_s is the associated static flow stress, the strain rate parameters C and P are called Cowper and Symonds constants. The failure strain of the mild steel is defined as 0.35. The material properties used in the calculation are given in Table 1.

3.4. BLAST LOAD MODELING

In this study, 1 kg TNT is detonated at a distance of 350 mm above the flat layer as illustrated in Figure 1. The scaled distance is 0.35 m/kg$^{1/3}$. Blast load is generated by using keyword *LOAD BLAST ENHANCED (LBE) via the CONWEP feature in Ls-Dyna [14]. As shown in Figure 4, the peak reflected overpressure is around 82.3 MPa. The keyword *LOAD BLAST ENHANCED considers the enhancement of reflected waves. The incident and reflected

Table 1. Material properties of 1045 steel (18)

Property	Young's Modulus	Poisson's Ratio	Yield Stress	Tangent Modulus	Density	Hardening Parameter, β	C	P
Value	203 GPa	0.3	507 MPa	3350 MPa	7850 Kg/m^3	1	40 s^{-1}	6

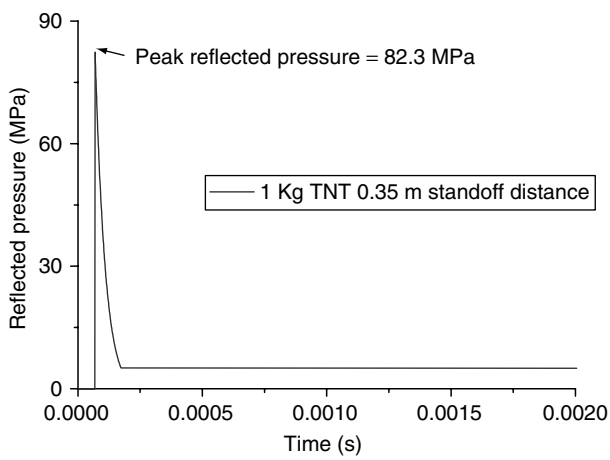

Figure 4. Reflected pressure time histories

pressures on the plate are hereby determined based on the amount of TNT, the standoff distance and angle of incidence [14]. It should be noted that the current results are obtained by calculating the blast loadings from empirical formulae in Ls-Dyna. Blast wave structure interaction is not considered although the reflecting blast pressure might be concentrated due to the arches channeling the blast waves. Detailed investigation into this phenomenon involves modeling blast wave propagation and interaction with structures, and is not carried out herein.

3.5. RESULTS AND DISCUSSIONS

The response quantities including peak displacement, amount of internal energy absorption, boundary reaction forces and plastic strain are compared. As shown in Table 2, adding stiffeners results in an increase in the peak and permanent displacements of the front arched layer and the peak displacement of the internal flat layer, but the permanent displacement of the flat layer of the panel "F4" is 7.2 mm, 50.3% less than that of the unstiffened panel "UU". This is because the thickness of the both layers of F4 is thinner than that of panel UU, therefore the two layers of F4 experience larger deformations, but the elastic response recovery of the stiffeners leads to partial reduction of the plastic responses of the two layers in F4. Because the permanent displacement of the internal layer of F4 is 50.3% less than that of UU, stiffened panel F4 has a better protection of internal contents.

Table 3 shows that the total internal energy (Et) and the internal energy of arched layer (Ei-1) of the stiffened panel are higher than the unstiffened panel subjected to blast loadings. This is because the thicknesses of the layers of the stiffened panel are reduced to make the total weight approximately the same as the unstiffened panel. Thus the thinner arched layer experiences more deformation which results in more internal energy absorption. Similarly the internal flat layer of the stiffened panel experiences less deformation and hence less internal energy absorption (Ei-2) than that of the unstiffened panel. Furthermore, the deformation of stiffeners (Ei-3) also takes some share of total internal energy. Figure 5 shows the time history of the total energy absorption (Et), internal energy (Ei-1, Ei-2, Ei-3) and the kinematic energy (Ek-1, Ek-2, Ek-3) absorbed by both layers and stiffeners of the panel "F4".

As illustrated in Figure 6 above, the schematic diagram of four edges and the reaction forces on the edges. The reaction forces in the X direction (Fx) mainly act on the edge 1 and 3. The

Table 2. Specification of panels and displacement of both layers

	Specification			**Displacement**				
	Stiffener Size	**Total weight**	**Thickness of layers**	**Arched Layer (mm)**		**Flat Layer (mm)**		
Panel	**(width*depth)**	**Kg**	**mm**	**Peak**	**Permanent**	**Peak**	**Permanent**	**Reduction**
UU	–	10.09	2.00	14.1	8.5	16.7	14.5	–
F4	10*5	10.09	1.39	20.9	14.5	19.0	7.2	50.3%

Table 3. Internal energy, reaction forces and plastic strain

	Internal Energy (KJ)			**Reaction Force (10^5N)**							
	Ei-1	**Ei-2**	**Ei-3**	**E**		**Redu-**		**Redu-**		**Redu-**	**Plastic**
Panel	**(arched)**	**(flat)**	**(stiffener)**	**(Total)**	**Fx**	**ction**	**Fy**	**ction**	**Fz**	**ction**	**Strain**
UU	5.5	3.4	–	9.4	2.19	–	2.94	–	2.06	–	0.270
F4	5.7	2.1	2.4	10.4	2.13	2.7%	2.49	15.3%	1.78	13.6%	0.120

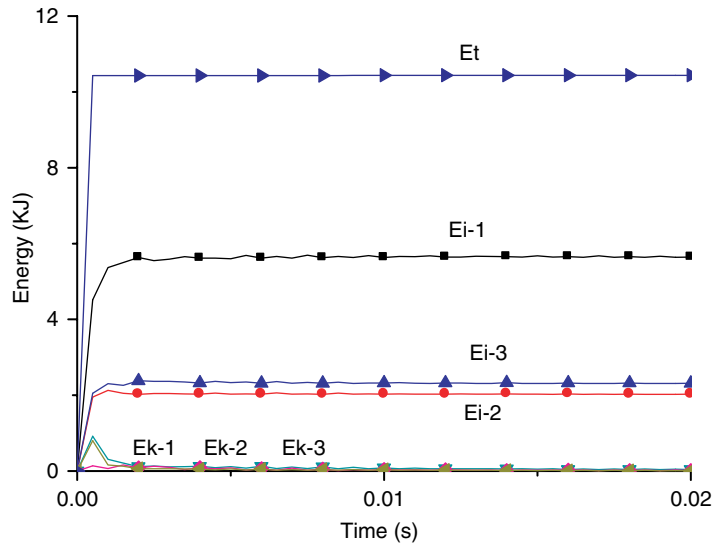

Figure 5. Energy time histories of panel F4

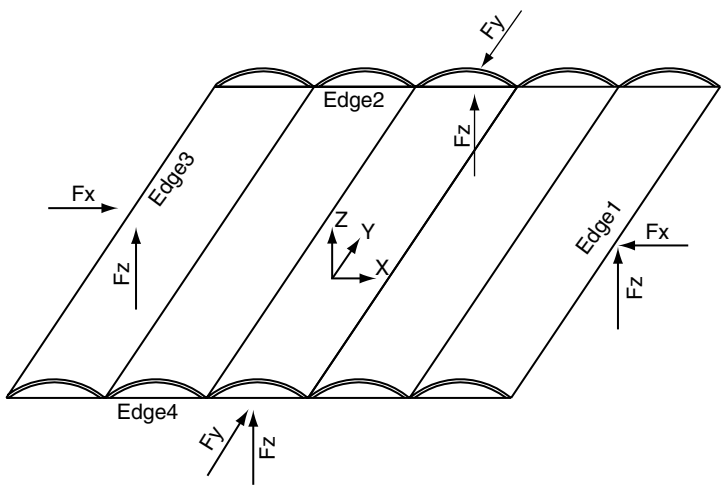

Figure 6. Schematic diagram of four edges and reaction forces Fx\Fy\Fz

reaction forces in the Y direction (Fy) mainly act on the edge 2 and 4. The reaction forces in the Z direction (Fz) act on all four edges. As shown in Table 3, the stiffened panel "F4" is effective in reducing the reaction forces in all the three directions. This is because the stiffened panel cancels out more blast loadings at the springing lines of two adjacent arches, thus less force acting on the arched surface is transferred to the edges of the panels. This will substantially reduce the loading at the supports, thus greatly reduce the possibilities of support damage.

As shown in Figure 7(a), high plastic strain of the unstiffened panel "UU" occurs at the springing line where the arched layer is welded to the flat layer. The peak plastic strain of

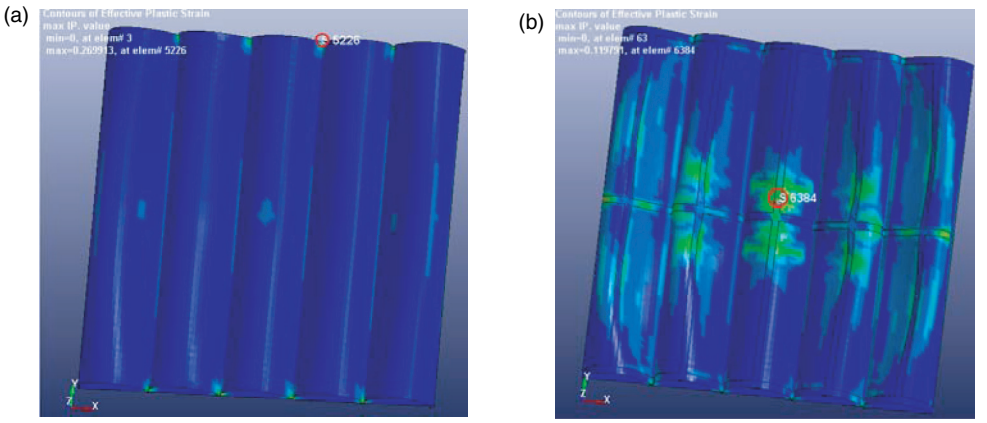

Figure 7. Plastic strain contours (a) unstiffened panel UU; (b) stiffened panel F4

0.270 occurs locally at the edge of the springing line (node 5226 indicated in Figure 7(a)) where the failure might happen. Therefore, the elements at these locations should be strengthened by placing the stiffeners. As shown in Figure 7(b), the peak plastic strain of the stiffened panel "F4" is decreased to 0.120 at node 6384 indicated in Figure 7(b), which is much lower than the failure strain of 0.35 of the steel material. This is because blast loading is distributed more evenly on the stiffened panel and the stiffeners also strengthen the weak locations. Therefore, placing the stiffeners strategically can greatly reduce the peak plastic strain of the panel, and hence reduce the damage potentials of the panel under blast loading.

In summary, the stiffened five-arch double-layered panel "F4" has been numerically demonstrated to perform better than the same weighted unstiffened panel in reducing the permanent displacement response of the internal plate, the reaction forces and the plastic strain, indicating a better system for blast panel design. However, the performance of the stiffened panels depends on the number, location and size of the stiffeners. Following presents parametric calculation results to derive the optimized stiffener designs for the five-arch double-layered panel.

4. PARAMETRIC STUDIES

This section presents parametric calculation results to study the influences of stiffener locations, sizes, number of stiffeners, boundary conditions, strain rate effect and blast intensity on the performance of stiffened five-arch double-layered panel to resist blast loading. The aim is to derive the optimal configurations of stiffeners that lead to better blast loading resistance capacity of the panel without increasing its weight. The response quantities including the peak displacement, the internal energy absorption, the boundary reaction forces and plastic strain are compared to determine the best performing panel.

The unstiffened panel "UU" is employed as a baseline for comparison purpose. A total of six panels with stiffeners arranged only on arched layer designated as "AU" to "FU" as shown in Figure 8, and another five panels with stiffeners on flat layer only, designed as "U1" to U5" as illustrated in Figure 11 are considered. The thicknesses of both layers are assumed the same and adjusted to make the total weight of all the panels approximately the same. All panels in parametric studies are subjected to 1kg TNT detonated at a distance of 350 mm above the internal flat layer.

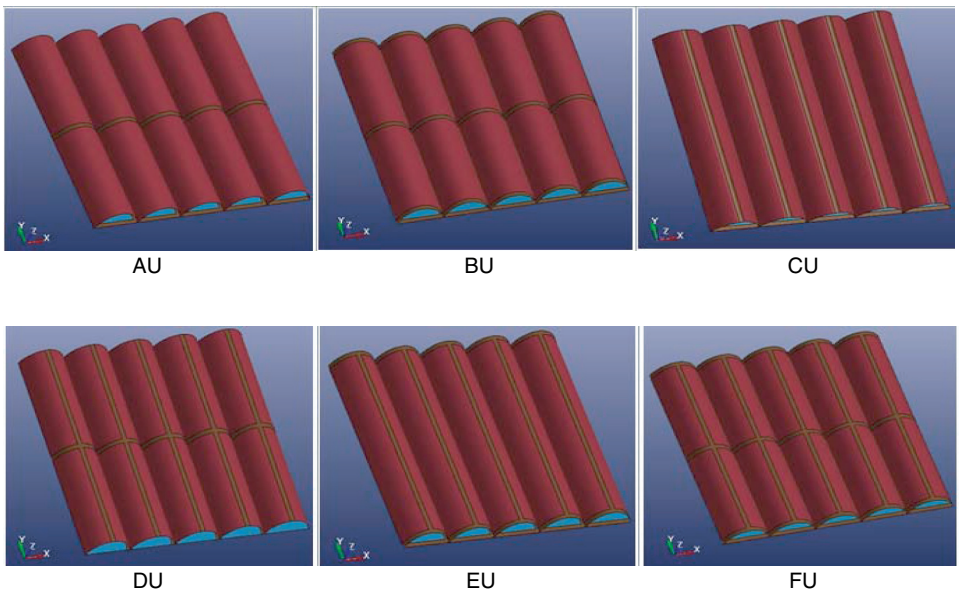

Figure 8. Six different stiffener arrangements on arched layer (AU-FU)

4.1. EFFECT OF STIFFENER ARRANGEMENTS ON ARCHED LAYER

Six stiffener arrangements ("AU-FU") on the arched layer are shown in Figure 8. A panel with one stiffener placed at the middle of arched layer in X direction is designated as "AU". A panel with three stiffeners placed at the middle and the two ends of the arched layer in X direction is designated as "BU". Panel "CU" has five stiffeners placed along the ridges of the arched layer in Y direction. Panel "DU" has five stiffeners along the ridges of the arched layer in Y direction and one stiffener at the middle of the arched layer in X direction. Panel "EU" also has five stiffeners along the ridges of the arched layer in Y direction and two stiffeners at the ends of the arched layer in X direction, and panel "FU", compared to panel "EU", has one more stiffener applied at the middle of the arched layer in X direction. The size of all the stiffeners is 10 mm in width and 10 mm in depth. To make the total weight of panels approximately the same as 10.09 kg, the thicknesses of layers are adjusted accordingly with the increase of the number of stiffeners. The corresponding thicknesses of the layers are given in Table 4. The boundary conditions of panels are assumed to be fully fixed around the perimeter of the flat layer.

Figure 9 (a) shows the deformation contour of the arched layer of the panel "FU". Table 5 shows the peak and permanent displacements of both layers of all the considered panels. The central point permanent displacements of the internal flat layer of all the stiffened panels except panel "EU" are smaller than that of the unstiffened panel "UU", indicating a better performance of those panels in protecting the interior objects. As can be noticed, applying stiffeners at the middle of the arch layer, even only one stiffener on each arch surface ("AU") results in a reduction in the permanent displacement of the internal flat layer. This is because stiffeners applied along the arch surface at the middle of the arched layer increase the arch stiffness and therefore reduce the displacement response of the layer. However, by comparing the displacement response of panels 'AU' and 'BU', and panels "CU" and 'EU", it is interesting to note that applying the stiffeners at the ends of the arch surface results in an increase in the displacement responses of the two layers, implying it is ineffective by

Table 4. Configurations of six stiffener layouts on arched layer

	Stiffeners on arched layer						
Panel	Length in Y (mm)	Pieces	Length in X (mm)	Pieces	Total length of stiffeners mm	Total weight Kg	Thickness of layers mm
UU	500	0	785	0	0	10.09	2.00
AU	500	0	785	1	785	10.09	1.88
BU	500	0	785	3	2356	10.09	1.63
CU	500	5	785	0	2500	10.09	1.61
DU	500	5	785	1	3285	10.09	1.49
EU	500	5	785	2	4071	10.09	1.37
FU	500	5	785	3	4856	10.09	1.24

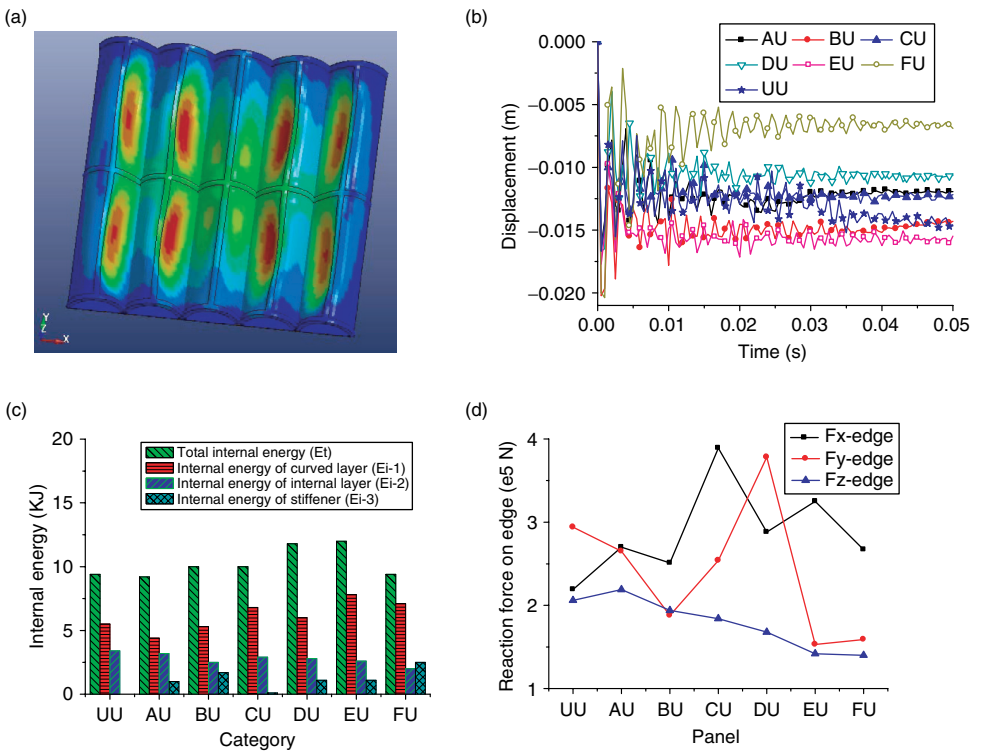

Figure 9. Influences of stiffener arrangements on arched layer (AU-FU): (a) Deformation contour of the panel "FU" (top view); (b) Displacement time histories at central point of the flat layer; (c) Internal energy absorptions; (d) Reaction forces on edges in X/Y/Z directions

using stiffeners at the two ends of the arch surface to mitigate displacement response of the layer. This is because the current study keeps all the panels approximately the same weight. Placing stiffeners results in thinner layers, which leads to larger panel center deformations. However, as shown in Table 6, applying stiffeners at the two ends is very effective in

Table 5. Displacements and internal energy (effect of stiffener arrangements on arched layer)

	Displacement					Internal Energy (KJ)			
	Arched Layer (mm)		Flat Layer (mm)						
Panel	Peak	Permanent	Peak	Permanent	Reduction	Ei-1 (arched)	Ei-2 (flat)	Ei-3 (stiffener)	E (Total)
UU	14.1	8.5	16.7	14.5	–	5.5	3.4	–	9.4
AU	11.6	7.5	16.3	12.0	17.2%	4.4	3.2	1.0	9.2
BU	18.0	13.0	20.2	14.5	0.0%	5.6	2.5	1.7	10.0
CU	13.9	7.5	16.4	12.5	13.8%	6.8	2.9	0.1	10.0
DU	15.1	8.3	16.7	10.5	27.6%	6.0	2.8	1.1	11.8
EU	12.5	9.5	17.7	15.6	–7.6%	7.8	2.6	1.1	12.0
FU	19.4	12.5	20.4	7.0	51.7%	7.1	2.0	2.5	9.4

Table 6. Reaction forces and plastic strain (effect of stiffener arrangements on arched layer)

	Reaction Force (10^5N)						
Panel	Fx	Reduction	Fy	Reduction	Fz	Reduction	Plastic Strain
UU	2.19	–	2.94	–	2.06	–	0.270
AU	2.70	–23.3%	2.65	9.9%	2.01	2.5%	0.253
BU	2.51	–14.6%	1.88	36.1%	1.94	5.8%	0.110
CU	3.89	–77.6%	2.54	13.6%	1.84	10.7%	0.248
DU	2.88	–31.5%	3.78	–28.6%	1.68	18.4%	0.250
EU	3.25	–48.4%	1.53	48.0%	1.42	31.1%	0.109
FU	2.67	–21.9%	1.59	45.9%	1.40	32.0%	0.115

reducing the support reactions. The panels "DU" and "FU" have the permanent displacements at the central point of the flat layer 10.5 mm and 7 mm, respectively, which are 27.6% and 51.7% less than that of the unstiffened panel. This is because the stiffeners are placed at the middle of the arch surface in both X and Y directions, which lead to more evenly distributed blast load to the whole arched layer, thus reduce the displacement at the center of the layer. The displacement time histories at the central point of the flat layer of the six panels subjected to blast loadings are shown in Figure 9 (b).

As shown in Figure 9 (c), the total internal energy (Et) and the internal energy of arched layer (Ei-1) of all stiffened panels except panel "AU" are higher than the unstiffened panel. This is again because the thicknesses of both layers are reduced to make the total weight approximately the same when placing the stiffeners on the arched layer. The thinner arched layer experiences more deformations which result in more internal energy absorptions. The internal energy of flat layer (Ei-2) of stiffened panels is less than that of the unstiffened panel because of their smaller deformation. The internal energy of stiffener (Ei-3) of panel "FU" is the highest among all stiffened panels simply because of the more number of stiffeners in this panel.

The reaction forces in X direction of all stiffened panels are higher than that of the unstiffened panel "UU". As shown in Figure 9 (d), the panel "CU" experiences 77.6% higher reaction force in X direction than that of the unstiffened panel. This is because the

unstiffened arched layer cancels more horizontal reaction forces along the springing lines. However, all the stiffened panels except "DU" experience lower reaction force in Y direction than the unstiffened panel. The panels "EU" and "FU" experience 48.0% and 45.9% lower reaction force in Y direction than the unstiffened panel. This is because the reaction forces along the springing lines distribute more evenly than that of the unstiffened panel through the stiffeners on the arched layer. Furthermore, all stiffened panels experience lower reaction force in Z direction than the unstiffened panel. The panels "EU" and "FU" perform better than others in reducing the reaction force in Z direction with reductions of 31.1% and 32.0%, respectively, indicating the demand on the support in Z direction will be reduced. This is because the arch surfaces of unstiffened panel cancel more horizontal reaction force at the springing lines but transferring larger vertical reaction forces.

As given in Table 6, the unstiffened panel experiences a peak plastic strain of 0.27. All stiffened panels experience lower plastic strains, especially "BU", "EU" and "FU", in which the largest plastic strains are 0.110, 0.109 and 0.115, respectively. However, the peak plastic strains for "AU", "CU" and "DU" are 0.253, 0.248 and 0.250, respectively, which are comparable to that of the unstiffened panel. Figure 10 shows the locations of peak plastic strains for unstiffened and stiffened panels which are highlighted by red circles. The peak plastic strains occur at the edges of arched layer for the panels "UU", "AU", "CU" and "DU" where there is no stiffener placed at the ends of arched layer in X direction. The panels "BU", "EU" and "FU" experience lower peak plastic strain which occurs around the middle of arched layer instead of the edges of arched layer, indicating the importance of placing stiffeners at the ends of arched layer in X direction. It can be concluded that the panels "BU", "EU" and "FU" perform better than other panels in terms of reducing the plastic deformations of the plate.

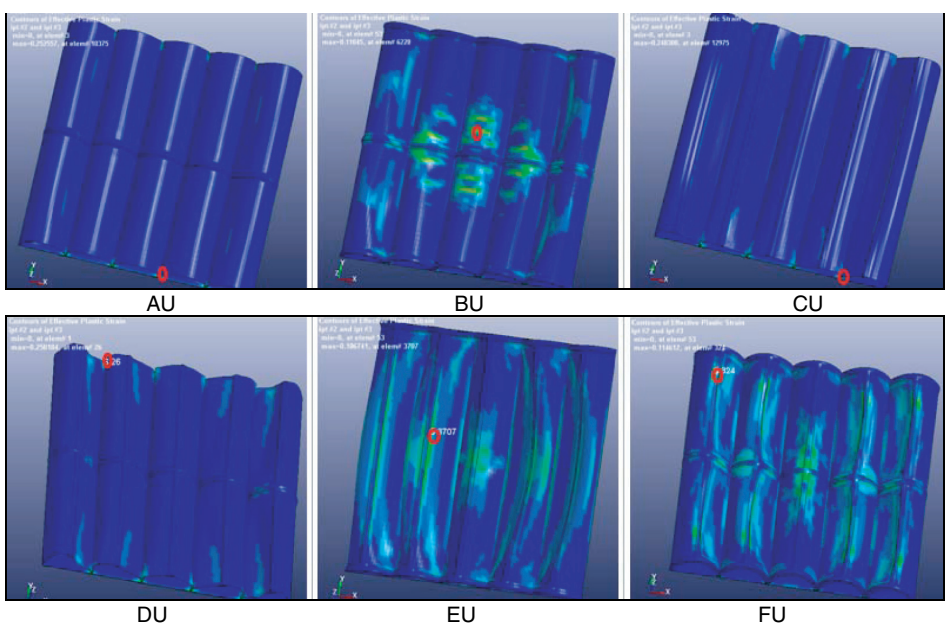

Figure 10. Plastic strain contours and locations of peak plastic strain of panels AU-FU

In summary, the stiffeners placed in the middle of the arched layer help to reduce the permanent displacement of the flat layer. The stiffeners placed at the ends of the arched layer help to reduce the peak plastic strain and the reaction forces in Y and Z directions.

4.2. EFFECT OF STIFFENER ARRANGEMENTS ON FLAT LAYER

Five stiffener arrangements (U1-U5) on the flat layer are considered in this section. The detailed layouts are shown in Figure 11. A panel with three stiffeners placed at the middle and ends of the flat layer in X direction is designated as "U1". A panel with four stiffeners placed at the springing lines of arch surfaces in Y direction is designated as "U2". A panel with four stiffeners placed at the springing lines of arches in Y direction and one stiffener at the middle of the flat layer in X direction is designated as "U3". A panel with four stiffeners at the springing lines of arches in Y direction and two stiffeners at the ends of flat layer in X direction is designated as "U4", and "U5" has four stiffeners at the springing lines of arches in Y direction and three stiffeners at the middle and ends of the flat layer in X direction. The sizes of the stiffeners are 10 mm in width and 10 mm in depth. To make the total weight of panels approximately the same as 10.09 kg, the thicknesses of the layers are adjusted accordingly with the number of stiffeners as given in Table 7. The boundary conditions of panels are assumed to be fully fixed around the perimeter of the flat layer.

Figure 12 (a) shows the deformation contour of the flat layer of the panel "U5". Table 8 gives the peak and permanent displacements of both layers of the considered panels. The displacement time histories at the central point of the flat layer of all panels subjected to blast loadings are given in Figure 12 (b). As shown, all the stiffened panels experience larger displacements than the unstiffened panel at the center point of the arched layer. This is because the thicknesses of the arched layers of all stiffened panels are thinner than that of the unstiffened panel "UU". However, the displacements of the flat layer of all the stiffened panels are smaller than the unstiffened panel. The panel "U4" experiences the smallest

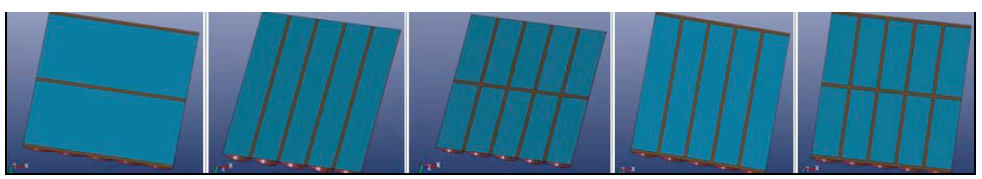

Figure 11. Five different stiffener arrangements on flat layer (U1-U5)

Table 7. Configurations of five stiffener layouts on flat layer

Panel	Stiffeners on flat layer		Total Length mm	Total weight Kg	Thickness of layers mm
	Length (mm)	Pieces			
UU	500	0	0	10.09	2.00
U1	500	3	1500	10.09	1.77
U2	500	4	2000	10.09	1.69
U3	500	5	2500	10.09	1.61
U4	500	6	3000	10.09	1.53
U5	500	7	3500	10.09	1.46

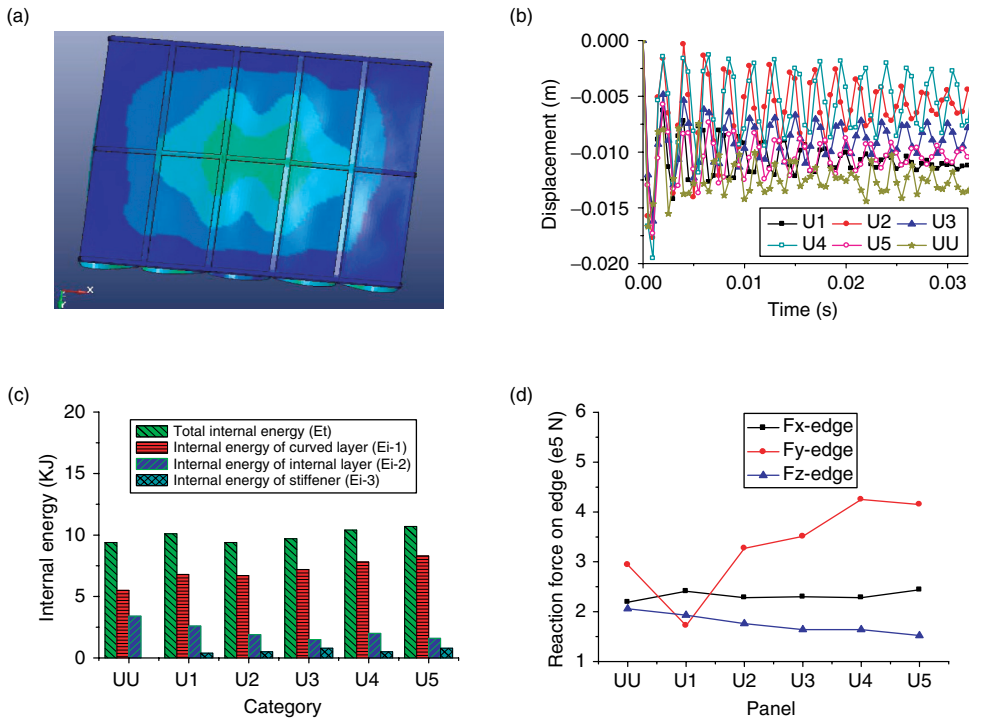

Figure 12. Influences of stiffener arrangements on flat layer (U1-U5): (a) Deformation contour of the panel "U5" (bottom view); (b) Displacement time histories at central point of the flat layer; (c) Internal energy absorptions; (d) Reaction forces on edges in X/Y/Z directions

Table 8. Displacements and internal energy (effect of stiffener arrangements on flat layer)

	Displacement					Internal Energy (KJ)			
	Arched Layer (mm)		Flat Layer (mm)						
Panel	Peak	Permanent	Peak	Permanent	Reduction	Ei-1 (arched)	Ei-2 (flat)	Ei-3 (stiffener)	E (Total)
UU	14.1	8.5	16.7	14.5	–	5.5	3.4	–	9.4
U1	27.1	18.0	17.7	10.8	25.5%	6.8	2.6	0.4	10.1
U2	32.1	22.5	16.2	7.0	51.7%	6.7	1.9	0.5	9.4
U3	33.3	23.0	19.5	9.0	37.9%	7.2	1.5	0.8	9.7
U4	37.3	27.0	17.3	6.0	58.6%	7.8	2.0	0.5	10.4
U5	39.4	29.0	19.7	10.5	27.6%	8.3	1.6	0.8	10.7

permanent displacement of 6.0 mm at the central point of the flat layer, which is 58.6% less than that of the unstiffened panel "UU". This is because the stiffeners placed on the flat layer increase the overall stiffness of the panel. The blast loads are more evenly distributed to the whole stiffened flat layer.

As shown in Figure 12 (c), the internal energy of arched layer (Ei-1) of all stiffened panels is higher than the unstiffened panel. This is because the thicknesses of both layers are reduced to make the total weight approximately the same. The thinner arched layers experience larger deformations which result in more energy absorptions. The stiffeners take little share of the total internal energy. The flat layer of all the stiffened panels absorbs less energy (Ei-2) than the unstiffened panel because of its smaller deformations.

Figure 12 (d) shows that the reaction forces in X direction of all the stiffened panels are slightly higher than that of the unstiffened panel. Similarly, the reaction forces in Y direction of all stiffened panels except panel "U1" are higher than that of the unstiffened panel. The panel "U4" and "U5" experiences 44.6% and 41.2% higher reaction force in Y direction than the unstiffened panel. This is because the stiffeners at the flat plate attract more forces owing to their relatively higher stiffness and transfer these forces to the supports. The panel "U1" experiences less reaction force in Y direction because no stiffener is placed in the Y direction at the springing lines of arches. However, the reaction forces in Z direction of all the stiffened panels are lower than that of the unstiffened panel because more blast loadings are carried in X and Y directions.

As shown in Table 9, all the stiffened panels experience lower plastic strain than the unstiffened panel. Especially, the panel "U3" experiences the lowest peak plastic strain of 0.112. Figure 13 shows the locations of peak plastic strains for the unstiffened and stiffened panels. The panel "U1" experiences the peak plastic strain at the edge of arched layer. This is because there is no stiffener placed at the springing lines of arches in Y direction. For all other stiffened panels, the peak plastic strains occur around the middle of arched layer where higher blast overpressure occurs. The above results indicate that the panel "U3" experiences the least damage as it has the smallest plastic strain among all the panels considered.

4.3. EFFECT OF STIFFENER SECTION SIZES

The panels "F4" with stiffeners of three different sections are considered to investigate the influence of stiffener sizes on panel performance. The dimensions of the three stiffener sections considered are 10 mm*5 mm, 5 mm*10 mm, 5 mm*5 mm (width*depth). The unstiffened panel "UU" with 2 mm thick layers is again used as the reference panel for comparison. Similarly, for the cases with the stiffener dimensions 10*5 mm and 5*10 mm, the panel thickness is changed to 1.39 mm in order to keep the overall panel weight unchanged. For the case with stiffener dimension 5 ∞ 5 mm, the panel thickness is also taken as 1.39 mm and the overall panel weight is therefore lighter as compared to the other cases. The dimension and weight of the example panels considered here are given in Table 10. The boundary of all the panels is assumed to be fully fixed around the perimeter of the internal flat layer.

Table 9. Reaction forces and plastic strain (effect of stiffener arrangements on flat layer)

	Reaction Force (10^5N)						Plastic Strain
Panel	**Fx**	**Reduction**	**Fy**	**Reduction**	**Fz**	**Reduction**	
UU	2.19	–	2.94	–	2.06	–	0.270
U1	2.41	–10.0%	1.72	41.5%	1.93	6.3%	0.159
U2	2.28	–4.1%	3.27	–11.2%	1.76	14.6%	0.144
U3	2.30	–5.0%	3.51	–19.4%	1.64	20.4%	0.112
U4	2.28	–4.1%	4.25	–44.6%	1.64	20.4%	0.150
U5	2.44	–11.4%	4.15	–41.2%	1.52	26.2%	0.137

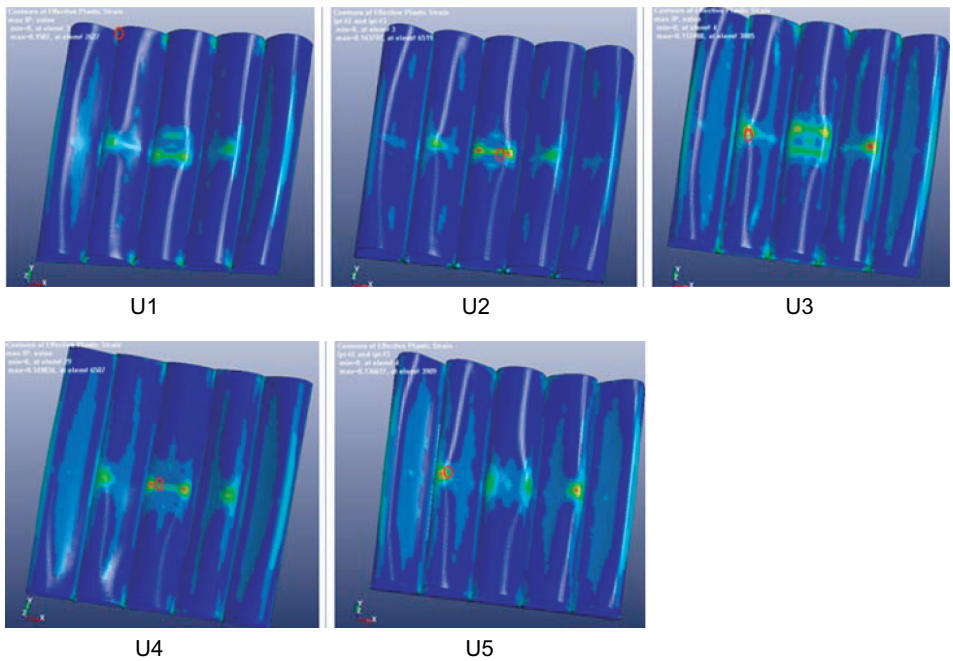

Figure 13. Plastic strain contours and locations of peak plastic strain of panels U1-U5

Table 10. Configurations of panels and displacements of both layers (effect of stiffener section sizes)

	Specification			Displacement				
	Stiffener section	Total weight	Thickness of layers	Arched Layer (mm)		Flat Layer (mm)		
Panel	(width*depth)	Kg	mm	Peak	Permanent	Peak	Permanent	Reduction
UU	–	10.09	2.00	14.1	8.5	16.7	14.5	–
10*5	10*5	10.09	1.39	20.9	14.5	19.0	7.2	50.3%
5*10	5*10	10.09	1.39	19.8	14.0	20.3	7.5	48.3%
5*5	5*5	8.55	1.39	29.0	21.5	22.0	10.5	27.6%

As shown in Table 10 and Figure 14, all stiffened panels have smaller permanent displacement at the central point of flat layer than the unstiffened panel. Among them, the panel with stiffener dimension "10*5 mm", has a permanent displacement of 7.2 mm, which is 50.3% lower than the unstiffened panel. It also has lower reaction forces in X/Y/Z directions than the unstiffened panel. The panel "5*10" has a permanent displacement of 7.5 mm, which is slightly higher than the panel "10*5", and higher reaction force in X direction but lower reaction forces in Y and Z directions than the unstiffened panel as given in Table 11. The panel "10*5" has a peak plastic strain of 0.120 and that of the panel "5*10" is 0.16 as shown in Figure 14. Figure 15 shows all the peak plastic strains occur at the middle of arched layer. These observations demonstrate that the stiffened panel "10*5" performs better among all the panels considered.

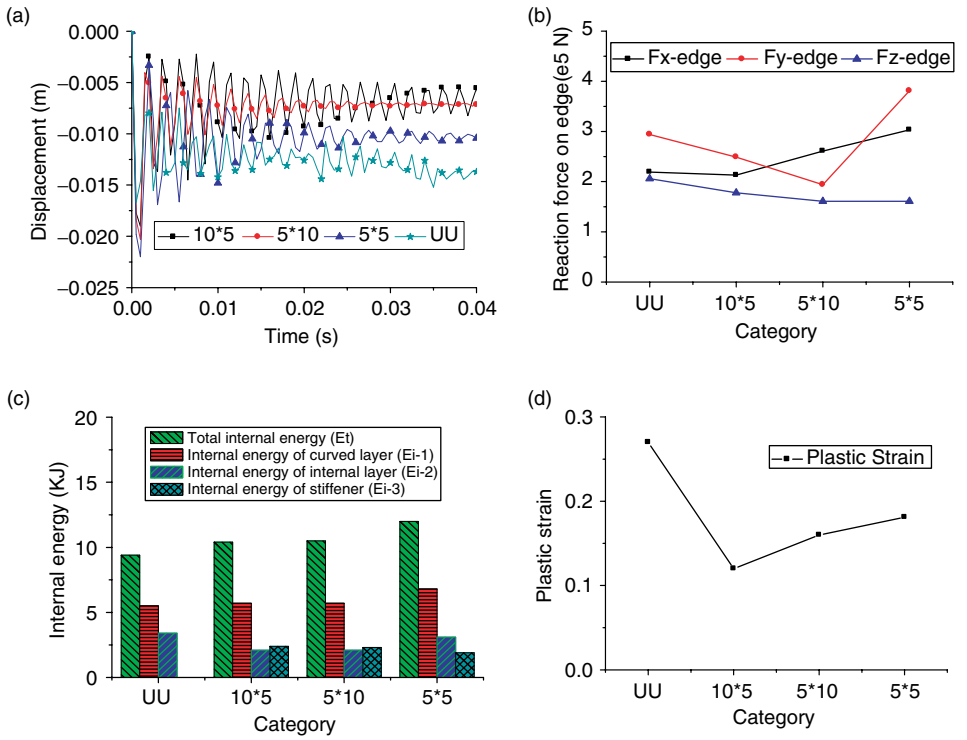

Figure 14. Influences of stiffener section sizes: (a) Displacement time histories at central point of the flat layer; (b) Reaction forces on edges in X/Y/Z directions; (c) Internal energy absorptions; (d) Peak plastic strains

Table 11. Internal energy, reaction forces and plastic strain (effect of stiffener section sizes)

	Internal Energy (KJ)				Reaction Force (10^5N)						Plastic Strain
Panel	Ei-1 (arched)	Ei-2 (flat)	Ei-3 (stiffener)	E (Total)	Fx	Reduction	Fy	Reduction	Fz	Reduction	
UU	5.5	3.4	–	9.4	2.19	–	2.94	–	2.06	–	0.270
10*5	5.7	2.1	2.4	10.4	2.13	2.7%	2.49	15.3%	1.78	13.6%	0.120
5*10	5.7	2.1	2.3	10.5	2.61	–19.2%	1.94	34.0%	1.61	21.8%	0.160
5*5	6.8	3.1	1.9	12.0	3.03	–38.4%	3.81	–29.6%	1.61	21.8%	0.181

4.4. EFFECT OF BOUNDARY CONDITIONS

Stiffened panel "F4" with five different boundary conditions is considered in this section to investigate the influences of different boundary conditions on panel responses to blast loadings. Five boundary conditions considered in the study are: 1) all the four edges fixed (designated as "4F"); 2) all the four edges pinned (designated as "4P"); 3) fixed on edges 1 & 2 & 3 and free on edge 4 (designated as "3F"); 4) fixed on edges 1 & 3 and free on edges 2 & 4 (designated as "2F"); 5) fixed on edges 2 & 4 and free on edges 1 & 3 (designated as "2FC"). The four edges of the panel are numbered and shown in Figure 6.

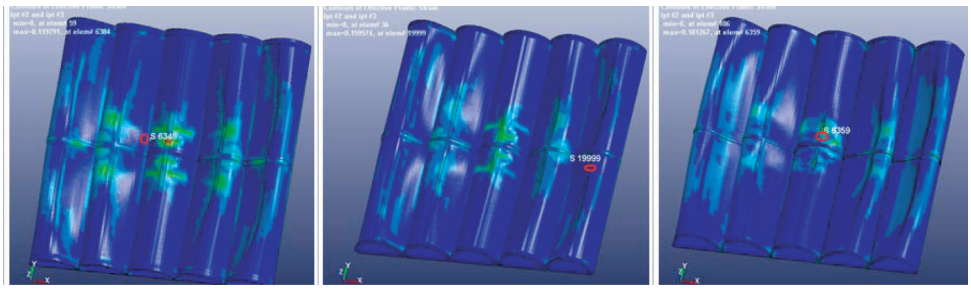

Figure 15. Plastic strain contours and locations of peak plastic strain of panels (effect of stiffener section sizes)

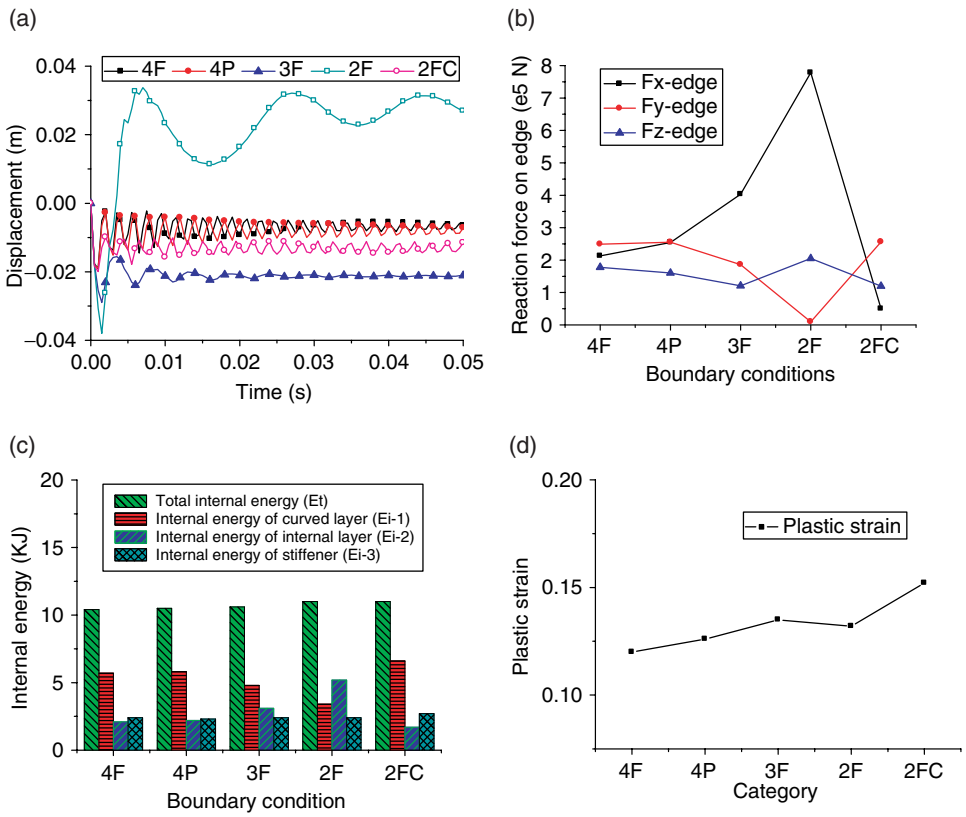

Figure 16. Influences of boundary conditions: (a) Displacement time histories at central point of the flat layer; (b) Reaction forces on edges in X/Y/Z directions; (c) Internal energy absorptions; (d) Peak plastic strains

The size of stiffener is 10 mm in width and 5 mm in depth. The thicknesses of both layers are 1.39 mm.

The displacement time histories at central point of the flat layer of the panel with five boundary conditions subjected to the blast loading are given in Figure 16 (a). Table 12 gives

Table 12. Specifications of panels and displacement of both layers (effect of boundary conditions)

	Specification			Displacement				
		Total weight	Thickness of layers	Arched Layer (mm)		Flat Layer (mm)		
Panel	Boundary Conditions	Kg	Mm	Peak	Permanent	Peak	Permanent	Reduction
4F	4 fixed on edge 1–4	10.09	1.39	20.9	14.5	19.0	7.2	–
4P	4 pinned on edge 1–4	10.09	1.39	21.6	15.0	19.0	8.0	–11.1%
3F	3 fixed on edge 1 & 2 & 3	10.09	1.39	25.7	17.2	29.0	21.0	–191.7%
2F	2 fixed on edge 1 & 3	10.09	1.39	38.4	20.0	38.0	33.7	–368.1%
2FC	2 fixed on edge 2 & 4	10.09	1.39	24.8	17.0	19.9	13.0	–80.6%

Table 13. Internal energy, reaction forces and plastic strain (effect of boundary conditions)

	Internal Energy(KJ)				Reaction Force (10^5N)						Plastic Strain
Panel	Ei-1 (arched)	Ei-2 (flat)	Ei-3 (stiffener)	E (Total)	Fx	Reduction	Fy	Reduction	Fz	Reduction	
4F	5.7	2.1	2.4	10.4	2.13	–	2.49	–	1.78	–	0.120
4P	5.8	2.2	2.3	10.5	2.54	–19.2%	2.55	–2.4%	1.60	10.1%	0.126
3F	4.8	3.1	2.4	10.6	4.03	–89.2%	1.86	25.3%	1.21	32.0%	0.135
2F	3.4	5.2	2.4	11.0	7.78	–265.3%	0.10	96.0%	2.05	–15.2%	0.132
2FC	6.6	1.7	2.7	11.0	0.50	76.5%	2.56	–2.8%	1.20	32.6%	0.152

the peak and permanent displacements of center points of both layers of the panel with five boundary conditions. The panel with boundary conditions "4F" and "4P" experience smaller permanent displacement of the flat layer than that with the other three boundary conditions. Release of one or two edges increases the permanent displacement. The panel with boundary condition "2FC" has better performance in terms of the permanent displacement than the panel with "3F" and "2F". It is worth noting that the panel with boundary condition "2F" experiences large peak displacement on the flat layer and the permanent displacement occurs in the positive or opposite direction of the blast loading, indicating the counter-intuitive behavior of the panel occurs. This is because the overall stiffness of the panel with boundary condition "2F" is much smaller than that of the panel with "2FC". Moreover, the reaction forces in X direction of the panel with "2F" and "3F" shown in Table 13 and Figure 16 (b) are much higher than the reaction forces in the other directions and in panels with other boundary conditions. The above results demonstrate the influences of boundary conditions on panel responses. Changing the boundary conditions of the panel might significantly affect the panel performances under blast loading.

As shown in Figure 16 (c), the arched layer of panel with boundary "2FC" has the highest internal energy (Ei-1) and its flat layer has the lowest internal energy (Ei-2) among all panels.

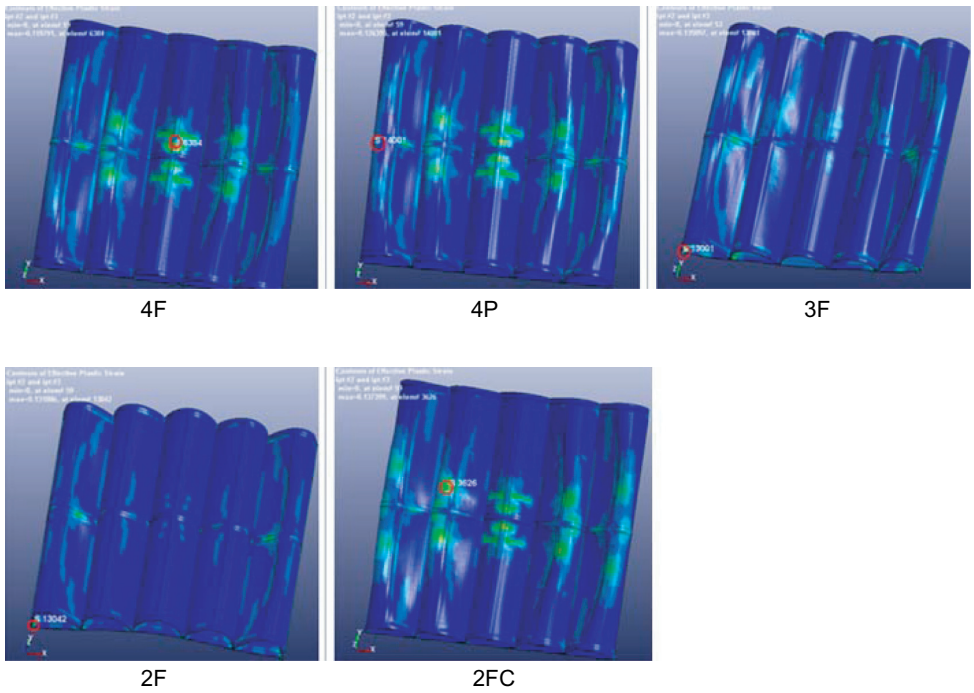

Figure 17. Plastic strain contours and locations of peak plastic strain of panels (effect of boundary conditions)

As shown in Figure 16 (d), the panel with "4P" experiences the lowest peak plastic strain of 0.120 while the panel with "2FC" has the highest peak plastic strain of 0.152. Figure 17 shows that the high plastic strains appeared at the edges of stiffeners for panels "3F" and "2F" whereas the high plastic strains more evenly distributed on the arched layer for panels "4F", "4P" and "2FC". The panels with boundary conditions "4P", "4F" and "2FC" perform better than the panels with other boundary conditions.

4.5. EFFECT OF STRAIN RATE SENSITIVITY

To demonstrate the strain rate effect, the model without considering strain rate effect is analyzed. All parameters are the same as those in Section 3 except the strain rate parameters C (Cowper constant) and P (Symonds constant) are both defined zero. As shown in Table 14, the model without considering strain rate effect experiences 240% higher peak central displacement than the model with considering strain rate effect. The model without

Table 14. Displacements of both layers and plastic strain (strain rate sensitivity)

	Arched Layer (mm)		Flat Layer (mm)			Plastic Strain
Panel	**Peak**	**Permanent**	**Peak**	**Permanent**	**Reduction**	
strain rate	20.9	14.5	19.0	7.2	–	0.120
no strain rate	36.0	32.0	28.8	24.5	–240.3%	0.156

considering strain rate effect also has higher peak plastic strain than the model that considers the strain rate effect. This is attributed to the increase of yield stress of material when strain rate effect is taken into account. This example demonstrates that the strain rate effect has great influence on the response to the blast loadings that neglecting it in the analysis may lead to inaccurate predictions of panel responses.

4.6. EFFECT OF BLAST INTENSITY

FEMA428 [19] presents four categories of terrorist bombing scenarios, i.e. luggage bomb, automobile bomb, van bomb and truck bomb. Their TNT equivalent weights are about 25 kg, 115 kg, 680 kg and 6800 kg, respectively. Their minimum stand-off distances have been identified from Figure 18 to ensure the safety of personnel and structures at certain levels.

To check the effectiveness of the stiffened multi-arch double-layered panel in resisting the blast loads from these terrorist bombing scenarios, four typical TNT charge weights (i.e., 25 kg, 115 kg, 680 kg and 6800 kg) at threshold standoff distances of 3 m, 6 m, 12 m and 29 m, respectively are considered. The size of stiffener is 10 mm in width and 5 mm in depth. The thicknesses of both layers are 0.6 mm. The boundary conditions of panels are assumed to be fully fixed around the perimeter of the flat layer. Figure 19 shows the reflected pressure time histories under different terrorist bombing scenarios considered in this study. The peak reflected pressures are 4.6, 2.7, 2.0 and 1.4 MPa and the reflected impulses are 399.4, 530.6, 848.9,1603.9 Ns, respectively; as given in Table 15.

As shown in Table 15 and Figure 20 (a), the peak and permanent displacement of arched and flat layers increases slightly with the rise of the peak reflected pressure, i.e from the

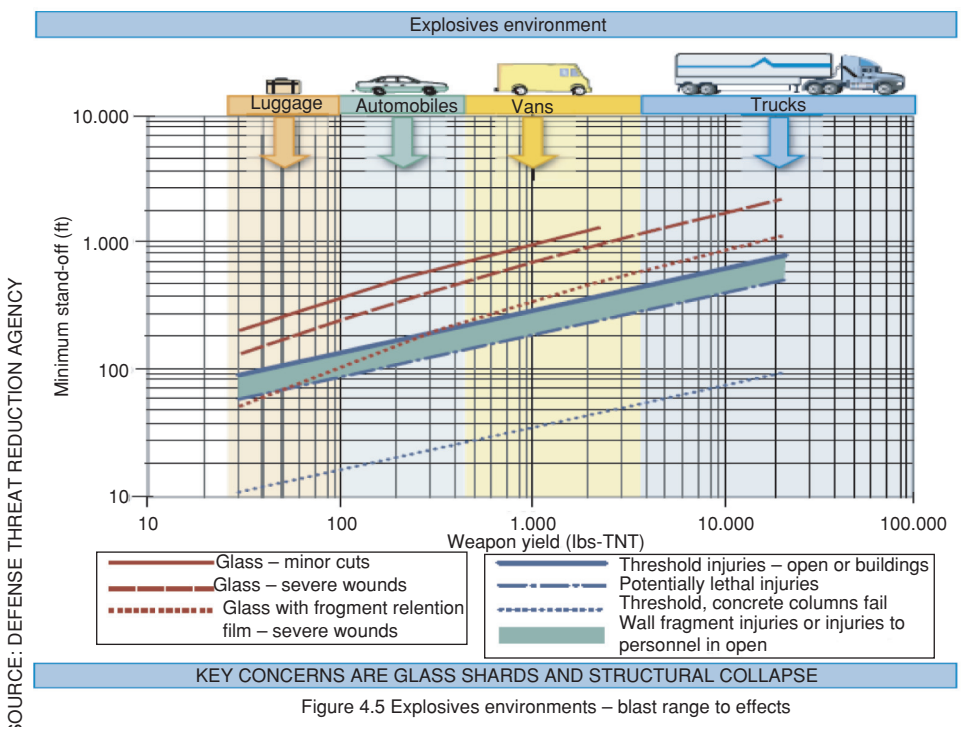

Figure 4.5 Explosives environments – blast range to effects

Figure 18. Terrorist bombing scenarios from FEMA428 (19)

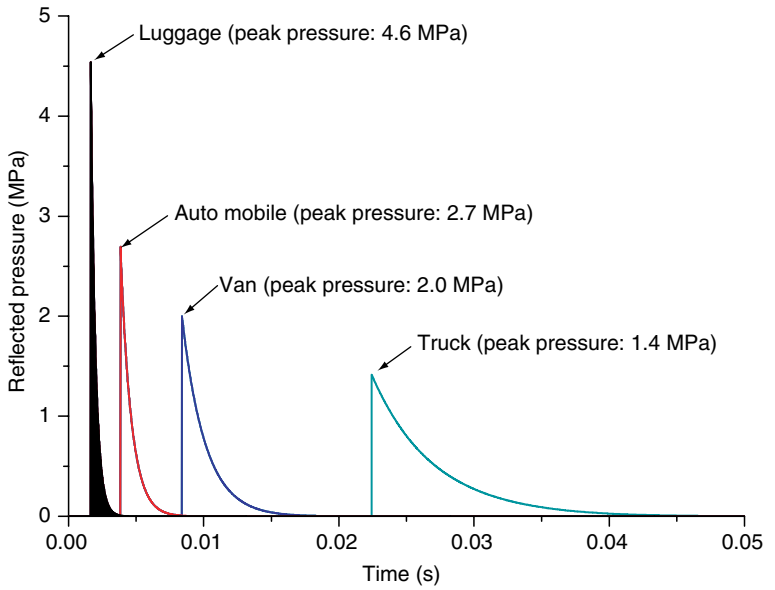

Figure 19. Reflected pressure time histories (different terrorist bomb scenarios)

Table 15. Displacements of both layers and plastic strain (effect of blast intensity)

		Peak		Displacement			
	Scale Distance	Reflected Pressure	Reflected Impulse	Arched layer (mm)		Flat layer (mm)	
Terrorist Bombs	m/kg^(1/3)	MPa	Ns	Peak	Permanent	Peak	Permanent
Luggage	1.03	4.6	399.4	21.4	12.5	22.5	11.0
Automobile	1.23	2.7	530.6	20.1	11.0	20.0	10.0
Van	1.36	2	848.9	21.2	12.5	21.1	11.2
Truck	1.53	1.4	1603.9	18.3	10.5	17.4	10.0

bombing scenario of truck to the scenario of luggage. However, when two bombing scenarios have close peak reflected pressure, such as the bombing scenarios of automobile and van, higher reflected impulse contributes to the larger displacement of both layers. Figure 20 (b) shows that the stiffened panel experiences the highest peak reaction forces under the bombing scenario of luggage, which is of the highest peak reflected pressure. As shown in Table 16 and Figure 20 (c, d), the energy absorbed by both layers and stiffners and the peak plastic strain increase with the rise of the peak reflected pressure. The panel under the bombing scenario of luggage experiences the highest peak plastic strain of 0.17. These results demonstrate that the responses of the stiffened panel mainly correlate with the peak reflected pressure, instead of the reflected blast impulse. Increasing the peak reflected blast pressure results in the rise of the deformation of both layers, the amount of total energy absorbed, the reaction force and the peak plastic strain.

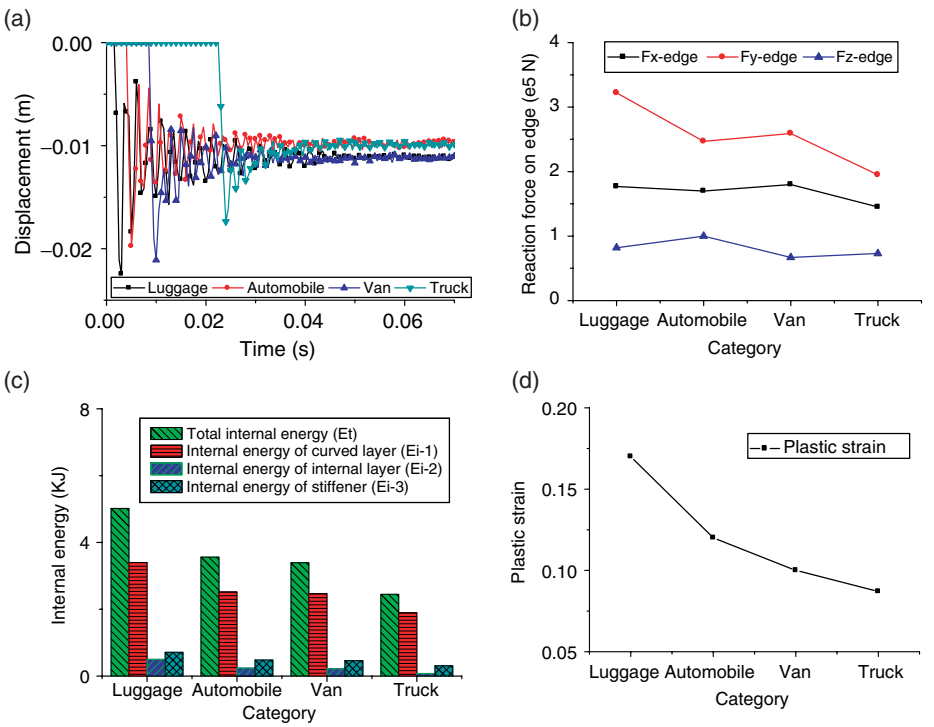

Figure 20. Influences of terrorist bombing scenarios: (a) Displacement time histories at central point of the flat layer; (b) Reaction forces on edges in X/Y/Z directions; (c) Internal energy absorptions; (d) Peak plastic strains

Table 16. Internal energy, reaction forces and plastic strain (effect of blast intensity)

	Internal Energy(KJ)				Reaction Force (10^5N)			Plastic Strain
Terrorist Bombs	Ei-1 (arched)	Ei-2 (flat)	Ei-3 (stiffener)	E (Total)	Fx	Fy	Fz	
Luggage	3.40	0.50	0.71	5.02	1.77	3.22	0.82	0.170
Automobile	2.52	0.24	0.48	3.56	1.70	2.47	1.00	0.120
Van	2.46	0.22	0.46	3.39	1.76	2.59	0.67	0.100
Truck	1.89	0.08	0.31	2.45	1.45	1.95	0.73	0.087

5. CONCLUSIONS

This study presents the numerical simulations of stiffened five-arch double-layered panels subjected to blast loading. The numerical results demonstrate that the stiffened five-arch double-layered panel with stiffeners placed strategically performs better than the unstiffened panel of the same weight in resisting blast loads. Parametric studies on the influences of different stiffener layouts, stiffener section size, boundary conditions, strain rate effect and blast intensity on the blast-resistant capacity are also carried out. The peak displacement, internal energy absorption, boundary reaction forces and the plastic strain are compared to

examine the effectiveness of various configurations on blast resistant capacity of the panel with stiffeners. It is found that the maximum structural response reduction of the stiffened five-arch panel depends on the strategic placement of stiffeners, appropriate boundary conditions and stiffener section sizes. The stiffened multi-arch panel has great application potential to mitigate blast loading effects in blast-resistant panel designs.

ACKNOWLEDGEMENTS

The authors acknowledge the partial financial support from Australian Research Council (ARC) to carry out this research work.

REFERENCES

[1] Chen W., Hao H., Numerical study of a new multi-arch double-layered blast-resistance door panel, *International Journal of Impact Engineering*, 43 (2012) 16–28.

[2] Anderson M., Dover D., Lightweight, Blast-Resistant Doors for Retrofit Protection Against the Terrorist Threat, 2nd *International Conference on Innovation in Architecture, Engineering and Construction* (AEC), Loughborough University, UK, 2003, pp. 23–33.

[3] Dharaneepathy M., Sudhesh K., Optimal stiffening of square plates subjected to air-blast loading, *Computers & Structures*, 36 (1990) 891–899.

[4] Nurick G.N., Olson M.D., Fagnan J.R., Levin A., Deformation and tearing of blast-loaded stiffened square plates, *International Journal of Impact Engineering*, 16 (1995) 273–291.

[5] Yuen S.C.K., Nurick G., Experimental and numerical studies on the response of quadrangular stiffened plates. Part I: subjected to uniform blast load, *International Journal of Impact Engineering*, 31 (2005) 55–83.

[6] Langdon G., Yuen S., Nurick G., Experimental and numerical studies on the response of quadrangular stiffened plates. Part II: localised blast loading, *International Journal of Impact Engineering*, 31 (2005) 85–111.

[7] Houlston R., Slater J., Pegg N., On analysis of structural response of ship panels subjected to air blast loading, *Computers & Structures*, 21 (1985) 273–289.

[8] Rudrapatna N., Vaziri R., Olson M., Deformation and failure of blast-loaded stiffened plates, *International Journal of Impact Engineering*, 24 (2000) 457–474.

[9] Goel M.D., Vasant A. Matsagar, Gupta A.K., Dynamic Response of Stiffened Plates under Air Blast *International Journal of Protective Structures*, 2 (2011) 139–156.

[10] Hsieh M.W., Hung J.P., Chen D.J., Investigation on the Blast Resistance of a Stiffened Door Structure, *Journal of Marine Science and Technology*, 16 (2008) 149–157.

[11] Pan Y., Louca L.A., Experimental and numerical studies on the response of stiffened plates subjected to gas explosions, *Journal of Constructional Steel Research*, 52 (1999) 171–193.

[12] Louca L., Punjani M., Harding J., Non-linear analysis of blast walls and stiffened panels subjected to hydrocarbon explosions, *Journal of Constructional Steel Research*, 37 (1996) 93–113.

[13] Grondin G., Elwi A., Cheng J., Buckling of stiffened steel plates—a parametric study, *Journal of Constructional Steel Research*, 50 (1999) 151–175.

[14] LSTC, LS-DYNA Version 971 Keyword User's Manual_Rev5-beta, Livermore Software Technology Corporation, 2010.

[15] Boyd S.D., Acceleration of a Plate Subject to Explosive Blast Loading-Trial Results, Defence Science and Technology Organisation, Australia, 2000, pp. 1–12.

[16] Hallquist J.O., Ls-Dyna® Theory Manual, Livermore Software Technology Corporation: Livermore, (2006).

[17] Theobald M.D., Nurick G.N., Numerical investigation of the response of sandwich-type panels using thin-walled tubes subject to blast loads, *International Journal of Impact Engineering*, 34 (2007) 134–156.

[18] Nakalswamy K.K. (2010). Experimental and numerical analysis of structures with bolted joints subjected to impact load. PhD Thesis, University of Nevada Las Vegas,

[19] FEMA, Primer to Design Safe School Projects in Case of Terrorist Attacks: Providing Protection to People and Buildings, Report 428, Federal Emergency Management Agency, Washington, 2003.